Acta of Bioengineering and Biomechanics
Vol. 16, No. 4, 2014

Original paper
DOI: 10.5277/ABB-00028-2014-02

Finite Element Analysis for Edge-to-Edge Technique to Treat Post-Mitral Valve Repair Systolic Anterior Motion

QI ZHONG[1,2], WENHUA ZENG[3]*, XIAOYANG HUANG[4], XIAOJIA ZHAO[4]

[1] Applied Mathematics School, Xiamen University of Technology, Xiamen, People's Republic of China.
[2] Cognitive Science Department, Xiamen University, Xiamen, People's Republic of China.
[3] Software School, Xiamen University, Xiamen, People's Republic of China.
[4] Computer Science Department, Xiamen University, Xiamen, People's Republic of China.

Systolic anterior motion of the mitral valve is an uncommon complication of mitral valve repair, which requires immediate supplementary surgical action. Edge-to-edge suture is considered as an effective technique to treat post-mitral valve repair systolic anterior motion by clinical researchers. However, the fundamentals and quantitative analysis are vacant to validate the effectiveness of the additional edge-to-edge surgery to repair systolic anterior motion. In the present work, finite element models were developed to simulate a specific clinical surgery for patients with posterior leaflet prolapse, so as to analyze the edge-to-edge technique quantificationally. The simulated surgery procedure concluded several actions such as quadrangular resection, mitral annuloplasty and edge-to-edge suture. And the simulated results were compared with echocardiography and measurement data of the patients under the mitral valve surgery, which shows good agreement. The leaflets model with additional edge-to-edge suture has a shorter mismatch length than that of the model merely under quadrangular resection and mitral annuloplasty actions at systole, which assures a better coaptation status. The stress on the leaflets after edge-to-edge suture is lessened as well.

Key words: *finite element modeling, mitral valve, edge-to-edge, systolic anterior motion*

1. Introduction

The mitral valve (MV), located between the left atrium (LA) and the left ventricle (LV), controls the blood flow from LA to LV. The mitral apparatus comprises four components: mitral annulus, two leaflets, i.e., anterior and posterior ones, chordae and two papillary muscles [7]. The chordae attach the leaflets to the two papillary muscles. Correct function of the mitral valve depends on the synergy of the four substructures and their proper mechanical behaviors. Mitral valve prolapse, a common valvular abnormality, is defined as prolapse of one or both of the mitral leaflets into LA, which is mostly caused by tissue myxomatous degeneration [10]. Mitral valvuloplasty attempts to repair the prolapsed valve and resume the valvular function. Systolic anterior motion (SAM) of the mitral valve is an unusual mitral complication of MV repair, which is known as the anterior motion of the anterior leaflet toward the septum and it induces left ventricular outflow tract obstruction (LVOTO) and mitral regurgitation. A redundant anterior leaflet is frequently related to post-mitral repair SAM [9].

Jebara et al. [11] reported that the incidence of post-repair SAM and LVOTO is reduced by combining posterior leaflet resection with a sliding plasty. However, Lee et al. [16] performing sliding plasty have had patients who had SAM developed. Triangular resection of the anterior leaflet as advocated by Grossi et al. [9] significantly diminished the incidence of SAM from 9.1% to 3.4%. Besides, Roberto et al. [19] prospectively used edge-to-edge technique to repair SAM, and the early and 2-year results were

* Corresponding author: Wenhua Zeng, School of Information Science and Engineering, Xiamen University, 361005 Xiamen. Tel: 08615969256926, e-mail: wenhuazeng@sina.cn
Received: April 24th, 2014
Accepted for publication: May 8th, 2014

satisfactory with total disappearance of SAM, of the LVOTO and of the mitral regurgitation.

Computational analysis of MV repair is a novel method to evaluate the effects of therapies on MV function. Finite element models not only reproduce the movement of the repaired valve, but also provide functional information on the stress state of the valve, which is an important factor to a surgery but imaging techniques cannot support. Kunzelman and colleagues [13] assessed mitral valve function after posterior chordal replacement with expanded polytetrafluoroethylene suture using finite element methods. And they also built models to compare the coaptation and stresses between the valve with flexible ring annuloplasty and the valve with rigid one [14]. Two commercial prostheses, the Physio ring and the Geoform ring, were compared by Votta et al. [23] using finite element modeling. They also showed that finite element models could be used to determine ring size after they simulated mitral annuloplasty on a patient-specific anatomy [21]. When it refers to edge-to-edge repair modeling, several groups have made investigation into this. Votta and colleagues [24] first simulated the edge-to-edge technology, and studied the importance of the suture position, length and depth. Lau et al. [15]., Dal Pan et al. [18] and Andrea et al. [3], [4] also engaged in finite element modeling of edge-to-edge repair. Lau et al. [15] took the blood into consideration and built fluid-structure interaction model. The functional and structural effects of percutaneous edge-to-edge double-orifice repair were studied as well, in comparison with traditional suture repair [4]. Recently, Tommaso et al. [17] developed patient-specific edge-to-edge models to apply finite element modeling to Mitral Clip intervention planning.

Among these present edge-to-edge repair finite element models, the material of the abnormal valve was always neglected, and the normal valve material models were used for the abnormal one. Nevertheless, the valve unable to coapt often suffers myxomatous degeneration which enhances extensibility and decreases stiffness of the valve leaflet and chordae [10]. The specific material model is necessary for myxomatous mitral valve. Otherwise, previous simulations were regularly based on anticipated repair therapy in order to obtain the optimal surgery plan. They were seldom based on the clinical surgery and rarely compared the models with actual outcomes.

In the present work, we attempted to simulate a specific clinical surgery procedure conducted by Roberto et al. [19] mentioned above using finite element methods, and quantitatively evaluate the edge-to-edge technique to treat post-mitral valve repair SAM. In our simulation, the geometry model of the mitral valve is in accordance with the pathology description of myxoid prolapsed mitral valve of the patients in [19], and the special mechanical property of the myxomatous mitral valve tissue was considered. The surgery actions such as quadrangular resection, mitral annuloplasty and edge-to-edge suture were simulated and their simulated results were compared with patient echocardiographic and operative data. The operation effect was evaluated by coaptation length and stress distribution on the leaflet model.

2. Materials and methods

In the clinical case of Roberto et al. [19], 4 patients requiring mitral valve repair surgery suffered chronic degenerative mitral regurgitation. Repair was first achieved through a quadrangular resection of the posterior leaflet and mitral annuloplasty with a ring. Routine perioperative transesophageal echocardiography showed SAM, sever LVOTO and mitral regurgitation. After resuming cardiopulmonary bypass, each patient had an additional edge-to-edge suture.

We generated the geometry of the uncorrected and corrected mitral valves by UGS NX software (Release 8.0). The structural dynamics of the mitral valve was simulated by the explicit finite element code LS-DYNA (Version: ls971d R5.0). Post-processing of the data was performed with LS-PREPOST.

2.1. Material model

The mitral valve of the patients in [19] suffers myxomatous degeneration. The mechanical properties of the myxomatous mitral valve leaflet have been characterized by Barber et al. [5], who tested the stress and strain of the myxoid valve leaflet tissue in radial and circumferential directions. We have presented an incompressible, hyperelastic constitutive model in [25] to characterize myxoid mitral leaflet tissue mechanics. The model incorporates the transversely isotropic response and the layered structure of the tissue. The Cauchy stresses of the two-layered composite in the first and second principal directions (σ'_{11} and σ'_{12}) can be written as follows:

when $\lambda_{f1} < \lambda^*_{f1}$,

$$\sigma'_{11} = c_1\left(\lambda_1^2 - \frac{1}{\lambda_1^2\lambda_2^2}\right) + r_1 c_2^1(\exp(c_3^1(\lambda_{f1}-1))-1)\cos^2\theta_1; \quad (1a)$$

when $\lambda_{f1} \geq \lambda_{f1}^*$,

$$\sigma'_{11} = c_1\left(\lambda_1^2 - \frac{1}{\lambda_1^2\lambda_2^2}\right) + r_1(c_4^1\lambda_{f1} + c_5^1)\cos^2\theta_1 + r_2(c_4^2\lambda_{f2} + c_5^2)\cos^2\theta_2; \quad (1b)$$

when $\lambda_{f2} < \lambda_{f2}^*$,

$$\sigma'_{22} = c_1\left(\lambda_1^2 - \frac{1}{\lambda_1^2\lambda_2^2}\right) + r_1 c_2^1(\exp(c_3^1(\lambda_{f1}-1))-1)\sin^2\theta_1 + r_2 c_2^2(\exp(c_3^2(\lambda_{f2}-1))-1)\sin^2\theta_2; \quad (2a)$$

when $\lambda_{f2} \geq \lambda_{f2}^*$,

$$\sigma'_{22} = c_1\left(\lambda_1^2 - \frac{1}{\lambda_1^2\lambda_2^2}\right) + r_1(c_4^1\lambda_{f1} + c_5^1)\sin^2\theta_1 + r_2(c_4^2\lambda_{f2} + c_5^2)\sin^2\theta_2; \quad (2b)$$

where $\lambda_{f1}^*, \lambda_{f2}^*$ are the stretches at which the collagen fibers in two layers are straightened. λ_1, λ_2, and λ_3, are the principal stretches. c_5^1 and c_5^2 can be determined from the condition that the exponential and linear regions are continuous at $\lambda_{f1}^*, \lambda_{f2}^*$.

$$c_5^1 = c_2^1(\exp(c_3^1(\lambda_{f1}^*-1))-1) - c_4^1\lambda_{f1}^* \quad (3a)$$

$$c_5^2 = c_2^2(\exp(c_3^2(\lambda_{f2}^*-1))-1) - c_4^2\lambda_{f2}^* \quad (3b)$$

In equatons (1a) and (1b) and equations (2a) and (2b), λ_1 and λ_2 are the principal stretches; λ_{f1} and λ_{f2} are the stretches in the two fiber directions. c_2^1, c_3^1, c_4^1 and c_5^1 are the material constants in the first layer, and c_2^2, c_3^2, c_4^2, and c_5^2 are the material constants in the second layer. These constants, determined by stress–strain data in [5] and listed in Table 1, were used in our material model.

Likewise, the mechanical properties of the myxoid chordae differ from that of the normal one. The modulus of the myxoid chordae is about 30 MPa which is almost one fifth of the normal chordae modulus calculated in [6].

In surgery simulation, the materials of the flexible ring of mitral annuloplasty and suture wire should be taken into consideration as well. The physical property of the ring is characterized by Young's modulus E = 2.544 MPa and coefficient of Poisson v = 0.45, as Kunzelman et al. described in [14]. Suture wire is made of polypropylene 4-0. The material has been considered elastic linear with Young's modulus E = 3500 MPa and coefficient of Poisson v = 0.38, based on [3].

2.2. Load and boundary condition

A time-dependent physiologic transvalvular pressure was applied on the surface of the leaflets [8] (shown in Fig. 1 and Fig. 2). It arises from the varying atrioventricular pressure during cardiac cycle. When comparing Fig. 1 and Fig. 2, we found that the maximum pressure of the LV in the case of mitral insufficiency is about 74 mm Hg which is lower than that of the valve fully closed (120 mm Hg), while the maximum pressure of LA in the mitral insufficiency case is higher. Herein, different time-dependent transvalvular pressures were applied to fully closed valve model and insufficiently closed one in our simulation.

The motion of the mitral annulus in myxomatous valve is not as significant as the normal valve, studied by Kaplan and colleagues [12]. Therefore, the mitral annulus in the model can be regarded to be immobile. As the papillary muscles kept the distance from the annulus, they can be considered fixed in cardio cycle as well.

2.3. Surgery procedure simulation

The simulation of the surgery procedure conducted by Roberto et al. [19] can be divided into three parts. We first developed the myxomatous valve model and mimicked its dynamics including prolapse status. Secondly, original repair was simulated by altering the

Table 1. Myxomatous leaflet material constants in equations (1a) and (1b) and equations (2a) and(2b)

Constants	c_1 (MPa)	c_2^1 (MPa)	c_3^1	c_4^1 (MPa)	c_2^2 (MPa)	c_3^2	c_4^2 (MPa)
value	3.00e-5	6.84e-3	8.83	6.57	1.47e-2	6.65	3.76

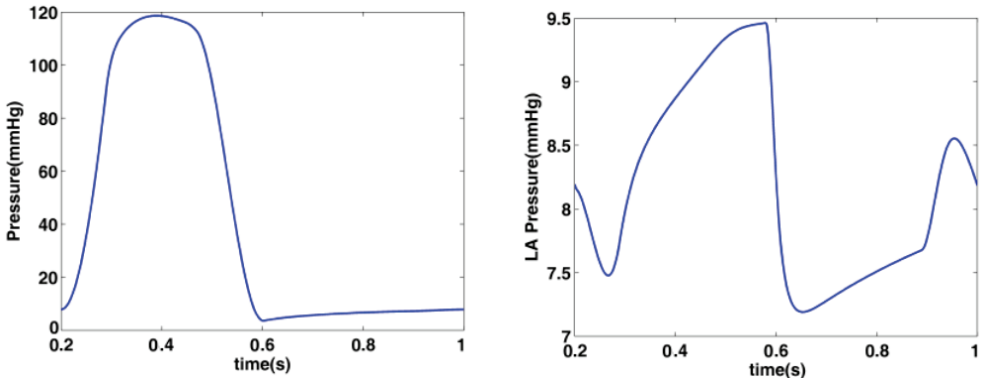

(a) (b)

Fig. 1. The time-dependent pressure of LV (a) and LA (b) in the case of mitral valve fully closed

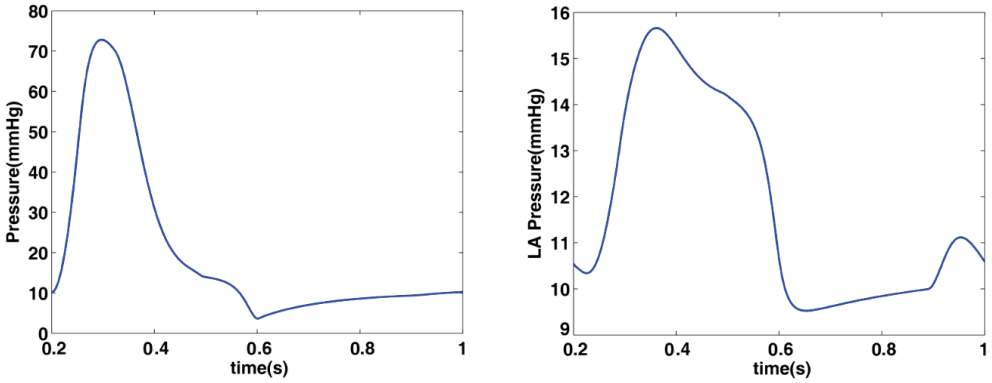

(a) (b)

Fig. 2. The time-dependent pressure of LV (a) and LA (b) in the case of mitral insufficiency

myxomatous valve model to apply quadrangular resection and mitral annuloplasty on it. Thirdly, based on the original repaired valve model, edge-to-edge suture was conducted as an additional repair. The dynamics of the valve under the two repairs above were also calculated.

2.3.1. Myxomatous mitral valve model

Following the dysfunctional mitral valve information of the patients in [19], the myxomatous mitral valve model was built. All patients had posterior leaflet prolapse with chordal rupture and they had large anterior leaflet with billowing. Thus, in our model (shown as Fig. 3), the chordae linking to posterior leaflet was eliminated and the anterior leaflet was heightened. Jeffrey et al. [20] advanced the size of the mitral annulus in myxomatous valve, so that was significantly increased especially in the interpeak span and we applied it in our model. Table 2 lists the detailed dimensional parameters of the myxomatous mitral valve model. The leaflet model

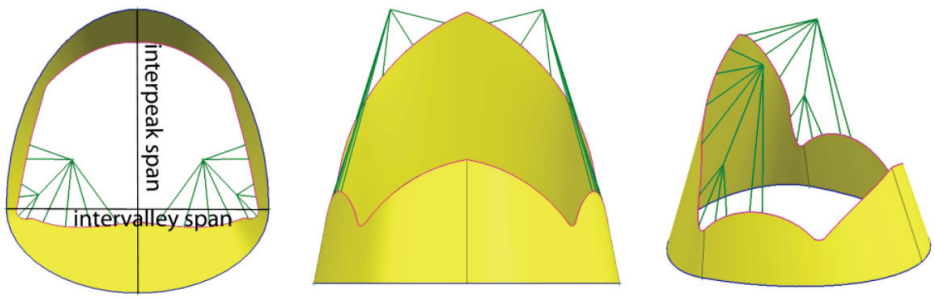

(a) (b) (c)

Fig. 3. 3D model of the mitral valve in a top view (a), a back view (b), and anisometric view (c)

Table 2. Dimensional parameters of the myxomatous mitral valve model

	Anterior leaflet height (mm)	Posterior leaflet height (mm)	Interpeak span (mm)	Intervalley span (mm)	Leaflet thickness (mm)	Annulus length (mm)
Value	30.3	13.8	35.0	32.0	2.0	106.4

is a bit thicker than the anatomy description of the normal leaflet attributed to the property of the myxoid leaflet [10].

2.3.2. Original repair model

The original repair was achieved by a quadrangular resection of the posterior leaflet and mitral annuloplasty with a ring inserted.

The quadrangular resection procedure involves removing a section of the posterior leaflet from the annulus to the free margin, and drawing the sides of the resulting gap closer and suturing the leaflet together[7]. The approach used for modeling this repair technique consisted first in cutting the nodes and elements on the section at the center of the posterior leaflet. And then the nodes on the cut line of the leaflet were selected to have displacement applied to them. Finally, these displacements drew the two lines together, and they met in the center of the removed section. Then, the suture lines joined the nodes over the gap. Figure 4 illustrates the process.

The ring used in the surgery is a complete semi-rigid CE Physio ring (Edwards Life-sciences, Irvine, CA), with an anterior saddle shape and progressive posterior flexibility [1]. The ratio between the intervallery span and the interpeak span is 4:3. Following these product descriptions, the artificial ring was modeled as a single profile line with certain ratio and shape. The ring model was discretized into 292 nodes. Mitral annuloplasty modeling was achieved via each annulus node moving to the nearest node on the ring.

2.3.3. Edge-to-edge repair model

The edge-to-edge repair involves joining two leaflets together and creating two small orifices. In the surgery of Roberto et al. [19], it was conducted after the complications, namely SAM and LVOTO, of the original repair appeared. All patients had a suture in

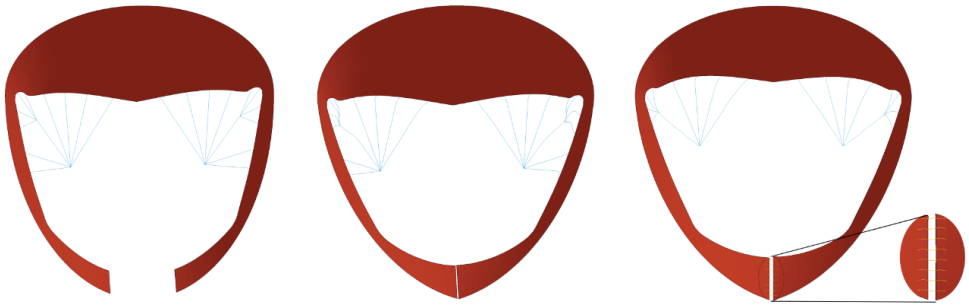

(a) (b) (c)

Fig. 4. Quadrangular resection simulation: (a) section removed, (b) section closed, and (c) gap sutured

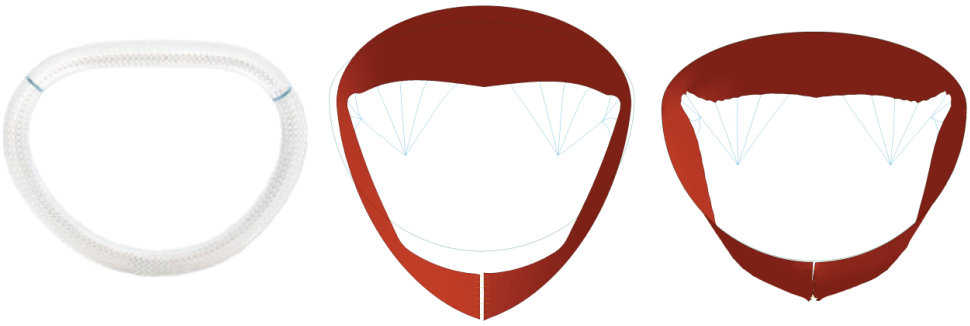

(a) (b) (c)

Fig. 5. Mitral annuloplasty simulation: (a) the image of the CE Physio ring;
(b) the model before annuloplasty, the green line denoting the artificial ring; (c) the model after annuloplasty

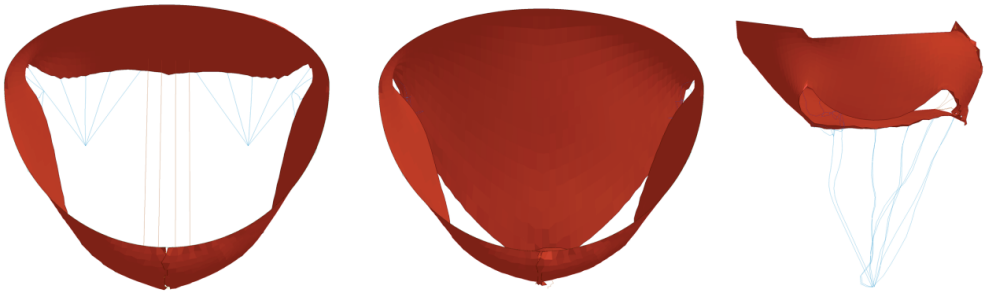

(a) (b) (c)

Fig. 6. Edge-to-edge repair simulation: (a) the model with suture joining the node on each leaflet; (b) and (c) are the two side views of the model when two leaflets close after beam contraction

the middle part of the free edge of the anterior and posterior leaflets. This short (5 mm) continuous suture took big bites into the leaflets assuring coaptation and reducing the tissue redundancy. The stitch was placed at the limit of the rough zone to force coaptation in this area, advocated by [2]. The suture procedure was simulated by first connecting the nodes on each leaflet over 5.4 mm on the border of the rough zone with spring beam element (k = 1000 g/mm). With the contraction of the beam according to their internal constitutive law and tension, the leaflets progressively close at the suture position.

3. Results

3.1. Closure dynamic

The present work simulated dynamics of mitral valve in the myxomatous model, original repair model and edge-to-edge repair model under transvalvular pressure during cardiac cycle.

Before surgery, the patient suffered serious mitral regurgitation (4 degree) and posterior leaflet prolapse. The myxomatous model simulated the prolapse process under the transvalvular pressure of mitral insufficiency at early systolic pressure ramp period when the anterior leaflet and posterior leaflet close to each other, as shown in Fig. 7. In normal condition, the valve should fully close at systolic peak, namely at t = 0.38 s here. However, the valve suffering prolapse in this case cannot close sufficiently with calculating regurgitation area of 8.9 cm^2. The posterior leaflet gradually closed to the annulus area, and eventually went beyond the annulus with the exceeding length of 5.4 mm, which was greater than the length threshold of the prolapse definition (2 mm) at systolic peak. The interpeak-span-velocity of the node on the edge of the posterior leaflet was 150.1 mm/s, and its velocity in the direction perpendicular to the annulus was 273.0 mm/s at t = 0.33 s.

After original repair, two leaflets contacted and did not prolapse to the atrial side any more, but there was a persistent aspect of redundancy of the anterior leaflet with SAM and LVOTO observed by routine post-repair transesophageal echocardiography and significant mitral regurgitation appeared after 2 to 10 minutes after de-clamping the aorta. Then edge-to-edge repair was done in clinic with the disappearance of the above symptoms. The valve dynamics were calculated under original repair and following edge-to-edge repair in our models. Figure 8 shows the closure process of the valve model when the transvalvular pressure gradually went up to the maximum. The original surgery simulation shows regurgitation area being greatly

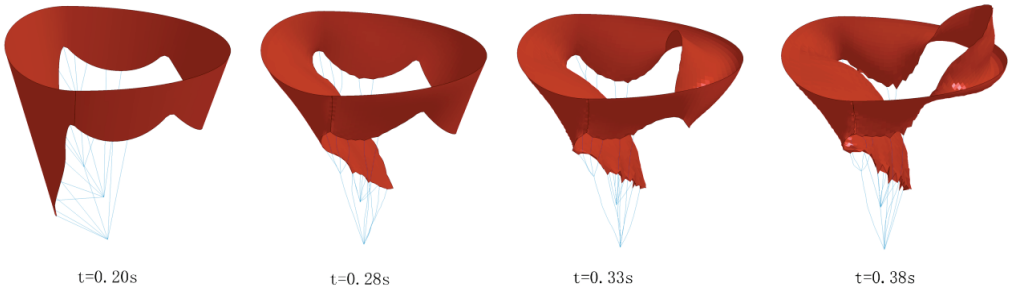

Fig. 7. The simulation of the prolapse process before surgery at four successive time points

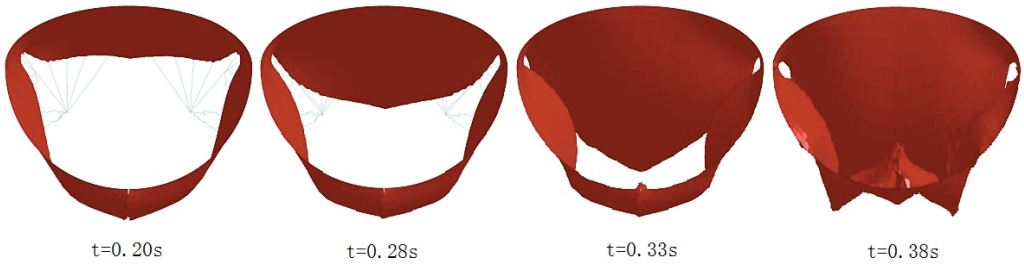

Fig. 8. The simulation of the coaptation process after the original repair at four successive time points

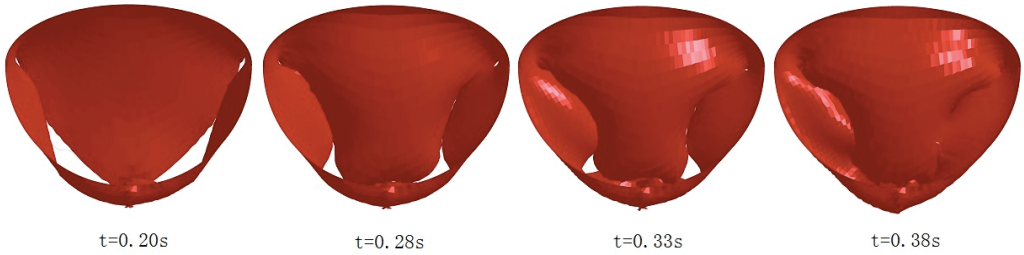

Fig. 9. The simulation of the coaptation process after the secondary repair at four successive time points

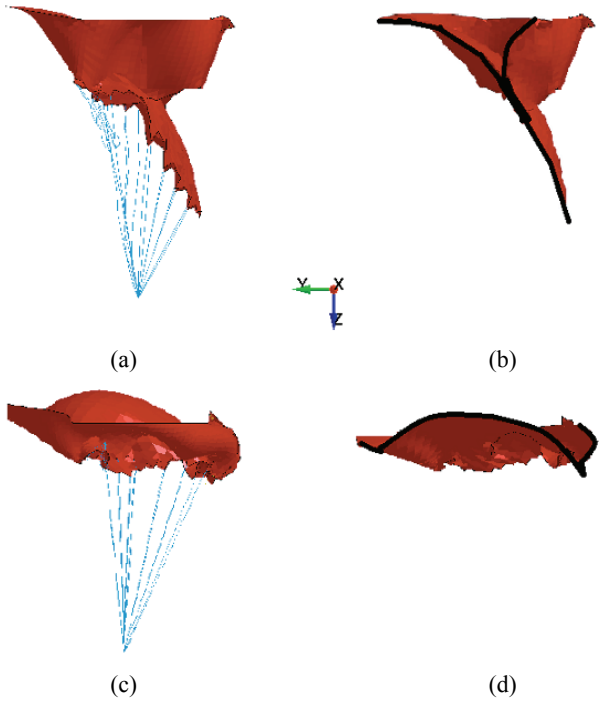

Fig. 10. Valve closure status under the maximum transvalvular pressure:
(a) and (c) are the side views of the valve model under original surgery and the one under edge-to-edge suture, respectively;
(b) and (d) are their leaflet half models. Black curve outlines the middle line of the leaflets

eliminated at the beginning and the leaflet prolapse disappeared.

The simulation of the edge-to-edge surgery displayed the valve to be fully closed with regurgitation area being zero at systolic peak (as shown in Fig. 9).

Figure 10 illustrates the valve closure status under the maximum transvalvular pressure, the edge-to-edge suture model shows the anterior leaflet edge coming into apposition with its counterpart on the posterior leaflet. However, the original repair model displays the posterior leaflet edge comes into the belly part of the anterior leaflet, namely, the anterior leaflet has much redundancy, which is consistent with the clinical surgery observation and the redundancy anterior leaflet is considered to be the reason of SAM and LVOTO.

In order to compare the coaptation quality of the valve models, the quantitative evaluation criterion of

coaptation defined by Votta et al. [23] was introduced. As shown in Fig. 11, L measure is assumed to be the length of the line from the beginning of the coapting tract to the leaflet free margin, which is divided into two terms: the length of the tract where leaflets are actually in contact (L_{coapt}) and the mismatch between the free margins of the two coapting leaflets (L_{fm}). The good coaptation model was defined as the one with long Lcoapt and short L_{fm}.

Table 3 lists the coaptation measurement of the two valve models. The valve model after original repair have longer L_{coapt}, but its L_{fm} is much longer than that of the edge-to-edge-repair model (0.73 mm).

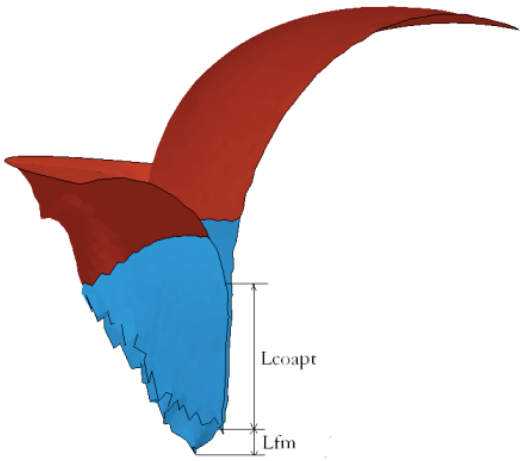

Fig. 11. Definition of the measured quantities of leaflets' coaptation in half model. Blue areas denote the rough zone of two leaflets. L measurement is equal to the sum of L_{coapt} and L_{fm}

Table 3. The coaptation measurement comparison between the original repair model and the edge-to-edge one

	Original repair model (mm)	Edge-to-edge repair model (mm)
L_{coapt}	4.58	2.27
L_{fm}	10.89	0.73

3.2. Leaflet stress

The leaflets in the model bore time-dependent transvalvular pressure during cardio cycle. The von Mises stresses calculated for the two leaflets were increasing with the pressure rise. As different time-dependent transvalvular pressures were applied to fully closed valve model and insufficiently closed one, we compared the von Mises stress distributions of the different valve models when they were under the same transvalvular pressure (7.92 kPa). The leaflets stress distributions of the models are illustrated in Fig. 12.

In the three models, the maximum stress is conformably observed near the annulus region; the bellies of the leaflets also experience high stress. The posterior leaflets carry fewer loads than the anterior leaflet in the myxomatous valve model and the edge-to-edge repair model. In the edge-to-edge repair model, the commissural areas also appear under high stress concentration. The maximum stress in the original repair valve model is up to 489.5 kPa, which is higher than that of the myxomatous valve model (377.3 kPa) and that of the edge-to-edge repair model (203.1 kPa).

4. Discussion

Through simulating a clinical surgery procedure, we obtained the quantitative information of the valves dynamics and stress distribution both before and after repairs. Our simulation demonstrated that the original repair including quadrangular resection and mitral annuloplasty prevented the leaflet from prolapsing toward the atrial side. The reason is that the original correct simulation has shorten the interpeak span of the valve, which enabled the anterior leaflet and the posterior one to meet each other and avoid the leaflet

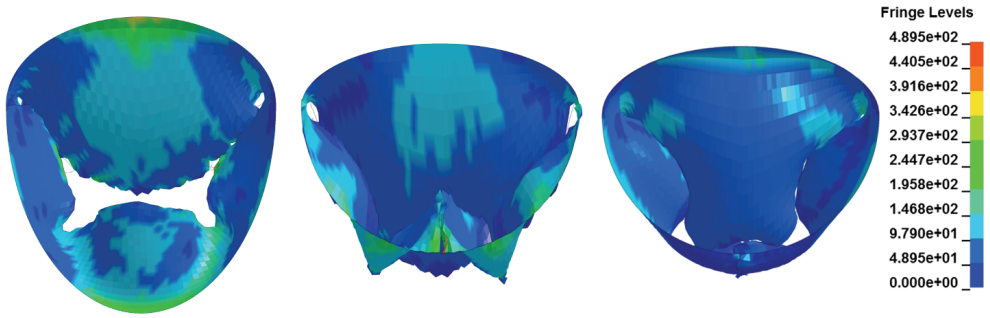

(a) (b) (c)

Fig. 12. Leaflets' von Mises stress distributions for the myxomatous valve model (a), the original repair model (b) and the edge-to-edge model (c)

prolapsing. However, the original correct simulation also shows that this repair could not make the valve close fully and perfectly with regurgitation area and long mismatch length (10.89 mm) owing to the redundant anterior leaflet. When the blood flowed toward LVOT, the redundant anterior leaflet would move to the septum reinforced by the Venturi effect and consequently lose the coaptation point inducing mitral regurgitation and LVOTO during systolic period [19]. The edge-to-edge technology sutured the two leaflets together, which restricted the anterior movement and made good coaptation with short mismatch length (0.73 mm), so as to successively eliminate existing mitral regurgitation, SAM and LVOTO. Furthermore, the comparison of the magnitudes of the von Mises stress calculated in the two repair models indicated that the edge-to-edge technology also reduced the loads carried by leaflet surface, which might guarantee the persistent validation of the edge-to-edge surgery.

Finite element models of the edge-to-edge repair developed by other authors always focused on the diastole period when the atrial pressure was larger than the ventricular one and the valve gradually opened. In order to compare our simulation result with others, we calculated the von Mises stress distribution on the leaflet when the transvalvular pressure reached the average value (0.52 kPa[15]) in diastole, as shown in Fig. 13a. The area near the suture zone on both leaflets bears high stress, which is consistent with the results of other models [3], [4], [15]. Differently, in the area near the center posterior annulus there appears stress distribution, which has not been found in other models [12], [14], [15] owing to the quadrangular resection in our simulation. The maximum stress on the leaflet in our model is about 121.5 kPa. When the transvalvular pressure was equal to 0.52 kPa, the orifice area was computed to be 2.9 cm^2, which was near the patients clinical measurement data (3.275 ± 0.325 cm^2) obtained by [19]. The suture tension predicted in our model was in the range between 0.05 N and 0.52 N, higher than the range of experimental data of 0.12–0.48 N reported in literature [22]. According to [18], the value of the suture tension in the edge-to-edge repair is always related to the suture length, depth and position and that may be the reason of the difference between the predicted suture tension and the experimental data.

5. Conclusions

Edge-to-edge technology is considered to be a solution to treat post-mitral valve repair SAM. In the present work, computational models were built to simulate a specific clinical surgery so as to demonstrate the validation of the edge-to-edge repair quantitatively. Models were developed based on the patient clinical measurement data and pathology description. The simulation result indicated that the edge-to-edge repair greatly restricted the movement of the anterior leaflet, guaranteed good coaptation and reduced loads carried by leaflets. The relief of SAM and LVOTO can attribute to these advantages of the edge-to-edge repair.

There still exist some limitations in the present study. Although the geometry of the mitral valve model stemmed from clinical data, the model and the patient nature valve were still different. For resuming the dynamics of nature valve dynamics, it is necessary to build the patient-specific model by 3D medical image data. In our work, the blood was not taken into consideration; LA and LV were neglected as well.

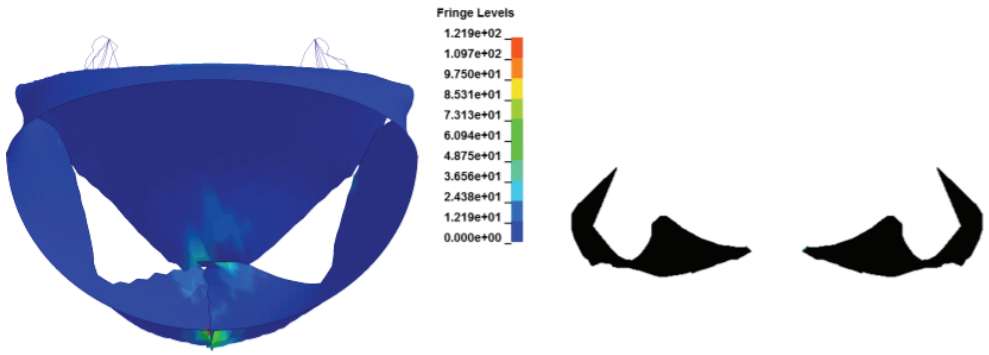

(a) (b)

Fig. 13. Valve deformation and von Mises stress distribution when the transvalvular pressure was equal to 0.52 kPa as viewed from 60 degree angle to the annulus plane (a); (b) is a profile of the whole orifice area at that time

These two simplifications limited the simulation of the anterior leaflet movement toward the septum under the blood flow which induced post-mitral valve repair SAM and LVOTO.

Model personalization is a big challenge for mitral valve repair simulation using finite element method, but this in-vitro and noninvasive method is very attractive for researchers to study the effects of therapies on mitral valve function. Finite element modeling may become a useful tool for mitral valve repair planning in the near future.

Acknowledgements

We gratefully acknowledge support from the National Natural Science Foundation of China (No. 61102137, 61271336, 61327001).

References

[1] *Carpentier-Edwards Physio Annuloplasty Ring*. Available: http://www.edwards.com/prod; ucts/rings/pages/physio.aspx

[2] ALFIERI O., MAISANO F., BONIS M.D. et al., *The double-orifice technique in mitral valve repair: a simple solution for complex problems*, J. Thorac. Cardiov. Sur., 2001, 122, 674–681.

[3] AVANZINI A., *A Computational Procedure for Prediction of Structure Effects of Edge-to-Edge Repair on Mitral Valve*, J. Biomech. Eng., 2008, 130, 031015-1-031015-10.

[4] AVANZINI A., DONZELLA G., LIBRETTI L., *Functional and structural effects of percutaneous edge-to-edge double-orifice repair under cardiac cycle in comparison with suture repair*, P. I. Mech. Eng. H, 2011, 225, 959–971.

[5] BARBER J.E., KASPER F.K., RATLIFF N.B. et al., *Mechanical properties of myxomatous mitral valves*, J. Thorac. Cardiov. Sur., 2001, 122.

[6] BARBER J.E., RATLIFF N.B., COSGROVE D.M. et al., *Myxomatous mitral valve chordae*. I: *Mechanical properties*, J. Heart Valve Dis, 2001, 10, 320–324.

[7] DOMINIK J., ZACEK P., *Heart Valve Surgery: An Illustrated Guide*, Springer, 2010.

[8] FENG M., *Research on Electronic Modeling and Simulation of Mitral Insufficiency*, Xiamen University, 2013.

[9] GROSSI E.A., STEINBERG B.M., LEBOUTILLIER M.R. et al., *Decreasing incidence of systolic anterior motion after mitral valve reconstruction*, Circulation, 1994, 90, II195–197.

[10] Hayek E., Gring C.N., Griffin B.P., *Mitral Valve Prolapse*, The Lancet, 2005, 365, 507–518.

[11] JEBARA V.A., MIHAILEANU S., ACAR C. et al., *Left ventricular outflow tract obstruction after mitral valve repair. Results of the sliding leaflet technique*, Circulation, 1993, 88, II30–34.

[12] KAPLAN S.R., BASHEIN G., SHEEHAN F.H. et al., *Three-dimensional echocardiographic assessment of annular shape changes in the normal and regurgitant mitral valve*, Am. Heart J., 1999, 139, 378–387.

[13] KUNZELMAN K., REIMINK M.S., VERRIER E.D. et al., *Replacement of mitral valve posterior chordae tendineae with expanded polytetrafluoroethylene suture: a finite element study*, J. Cardiac. Surg., 1996, 11, 136–145.

[14] KUNZELMAN K.S., REIMINK M.S., R.P. C., *Flexible versus rigid ring annuloplasty for mitral valve annular dilation: a finite element model*, J. Heart Valve Dis, 1998, 7, 108–116.

[15] LAU K., DÍAZ-ZUCCARINI V., SCAMBLER P. et al., *Fluid-structure interaction study of the edge-to-edge repair technique on the mitral valve*, J. Biomech., 2011, 2409–2417.

[16] LEE K.S., STEWART W.J., SAVAGE R.M. et al., *Systolic anterior motion of mitral valve after the posterior leaflet sliding advancement procedure*, Ann. Thorac. Surg., 1994, 57, 1338–1340.

[17] MANSI T., VOIGT I., GEORGESCU B. et al., *An integrated framework for finite-element modeling of mitral valve biomechanics from medical images: Application to MitralClip intervention planning*, Med. Image Anal., 2012, 16, 1330–1346.

[18] PAN F.D., DONZELLA G., FUCCI C. et al., *Structural effects of an innovative surgical technique to repair heart valve defects*, J. Biomech., 2005, 38, 2460–2471.

[19] ROBERTO M., AL A.N., MAURO L. et al., *Edge-to-Edge Technique to Treat Post-Mitral Valve Repair Systolic Anterior Motion and Left Ventricular Outflow Tract Obstruction*, Ann. Thorac. Surg., 2005, 76, 471–474.

[20] SILBIGER J.J., *Anatomy, mechanics, and pathophysiology of the mitral annulus*, Am. Heart J., 2012, 164, 163–176.

[21] STEVANELLA M., MAFFESSANTI F., CONTI C.A. et al., *Mitral Valve Patient-Specific Finite Element Modeling from Cardiac MR: Application to an Annuloplasty Procedure*, Cardiovasc. Engineering Technol., 2011, 2, 66–76.

[22] TIMEK T.A., NIELSEN S.L., LAI D.T. et al., *Mitral annular size predicts Alfieri stitch tension in mitral edge-to-edge repair*, J. Heart Valve Dis., 2004, 13, 165–173.

[23] VOTTA E., MAISANO F., BOLLING S.F. et al., *The Geoform Disease-Specific Annuloplasty System: A Finite Element Study*, Ann. Thorac. Surg., 2007, 84, 92–101.

[24] VOTTA E., MAISANO F., SONCINI M. et al., *3-D computational analysis of the stress distribution on the leaflets after edge-to-edge repair of mitral regurgitation*, J. Heart Valve Dis., 2002, 11, 810–822.

[25] ZHONG Q., ZENG W., HUANG X. et al., *Constitutive modeling and finite element analysis of myxomatous mitral leaflet tissue*, J. Mech. Med. Biol., 2014, 14.